Silver(I) ions bridged by pyridazine: doubling the ligand functionality for the design of unusual 3D coordination frameworks†‡

Konstantin V. Domasevitch,*[a] Pavlo V. Solntsev,[a] Il'ya A. Gural'skiy,[a] Harald Krautscheid,[b] Eduard B. Rusanov,[c] Alexander N. Chernega[c] and Judith A. K. Howard[d]

Received 4th May 2007, Accepted 25th June 2007
First published as an Advance Article on the web 23rd July 2007
DOI: 10.1039/b706731c

Nitrogen donor tetradentate ligands 4,4′-bipyridazine (*bpdz*) and pyridazino[4,5-*d*]pyridazine (*pp*) were prepared by inverse electron demand Diels–Alder cycloaddition reactions of 1,2,4,5-tetrazine. Examination of their behaviour towards silver(I) ions revealed a special potential of the ligands for the design of 3D coordination frameworks involving characteristic polynuclear and polymeric silver(I)–pyridazine motifs and multiple coordination of the ligands. $Ag_4(pp)_5(ClO_4)_4$ and $Ag_4(pp)_5(SiF_6)(BF_4)_2{\cdot}4H_2O$ adopt a unique 3D trinodal 4,4,5-connected topology based upon five-fold coordination of the metal ions and tetradentate bridging function of the organic modules. Complexes $Ag_3(L)_3(SO_3CF_3)_3{\cdot}nH_2O$ and $Ag_4(L)_3(X)_4{\cdot}nH_2O$ (L = *bpdz*, *pp*; X = BF_4^-, $0.5SiF_6^{2-}$) illustrate formation of highly-connected frameworks incorporating trinuclear clusters as an origin of the net connectivity. In the carboxylate complexes $Ag_2(L)(R_FCOO)_2$ (R_F = CF_3, C_2F_5, C_3F_7) the pyridazine and acido ligands act as complementary linkers for generation of 3D frameworks involving helicate motifs. Fused bicyclic pyridazine *pp* is a unique system combining very efficient σ_N-donor ability and pronounced π-acidity. The coordination frameworks commonly exhibit strong anion–π interactions, including unprecedented examples of double anion–π,π binding that occur between pyridazino[4,5-*d*]pyridazine as a double π,π-receptor for geometry complementary SiF_6^{2-} anions.

Introduction

In recent years, development of metal–organic frameworks has been paid much attention considering versatile areas of their potential applications.[1–3] Therefore many approaches towards designing framework architectures[4–6] aimed at the preparation of rigid and chemically robust coordination lattices have been examined.[1,7,8] The latter are generally accessible using polydentate bridging ligands with multiple binding sites for coordination interactions, particularly for the systems that are based upon hybrid inorganic/organic interconnection of the metal ions and involving simpler inorganic motifs as subunits of the framework structure.[9,10] Recently, new versatile possibilities for the generation of coordination architectures were found with utilization of polynuclear metal–organic clusters as the augmented nodes of the net, which support very unusual structures of eight-[11–13] and twelve-connected frameworks.[14]

The applicable ligand systems generally offer donor sites for bridging of closely situated metal ions, as provided by carboxylates, 1,2-diazoles and 1,2-diazines, a family of paradigmatic species commonly sustaining a diversity of polynuclear motifs. However, the electronic factors may appreciably contribute to metal–ligand interactions in many such cases since N-heteroaromatic ligands are typically very soft bases favouring coordination to soft acids and the effects of back-bonding are also particularly prevalent.[15] One of the best complementary systems involves electron deficient N-heteroaromatic ligands, such as pyridazines, coordinated to soft copper(I) and silver(I) ions.[15–17] They adopt a variety of characteristic chains, helices,[18–20] cycles[21,22] and discrete polynuclear ensembles,[23–25] possessing as yet unexplored potential as "supramolecular synthons" for coordination polymers.

Therefore, especially rich possibilities for the design of three-dimensional metal–organic frameworks may be anticipated for the ligands combining two pyridazine functions (Scheme 1). The available multiple donor sites allow tetradentate coordination of the ligand to soft silver(I) ions with its four-fold immobilization within the entire connectivity and integration of typical pyridazine bridged silver(I) motifs into the 3D array. That the bifunctional pyridazine ligands unite the potential of small diazine linkers[18–26] and long-distance bitopic connectors of the 4,4′-bipyridine type,[4,16] suggests new and exclusively flexible approaches for supramolecular synthesis of framework solids. The ligand structure itself offers different ways for combining the set of

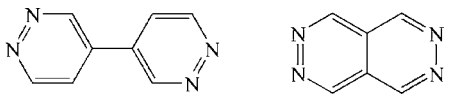

(4,4′-bpdz) *(pp)*

Scheme 1 Bifunctional pyridazine ligands explored in the present study.

[a]*Inorganic Chemistry Department, Kiev University, Volodimirska Str.64, Kiev, 01033, Ukraine. E-mail: dk@univ.kiev.ua*
[b]*Institut für Anorganische Chemie, Universität Leipzig, Linnéstraße 3, D-04103, Leipzig, Germany*
[c]*Institute of Organic Chemistry, Murmanskaya Str.4, Kiev, 253660, Ukraine*
[d]*Department of Chemistry, University of Durham, Durham, UK DH1 3LE*

† CCDC reference numbers 643960–643971. For crystallographic data in CIF or other electronic format see DOI: 10.1039/b706731c

‡ Electronic supplementary information (ESI) available: Details for organic syntheses, ORTEP drawings for structures **1**–**12**. See DOI: 10.1039/b706731c

pyridazine functions: either by coupling (4,4′-bipyridazine, *bpdz*) or annelation (pyridazino[4,5-*d*]pyridazine, *pp*). The annelation of a N-heteroaromatic ring decreases the LUMO energy comparably with the introduction of a strong electron-withdrawing substituent and hence the symmetric *d*-edge sharing of two pyridazine cycles yields an extremely electron deficient system. In this respect pyridazino[4,5-*d*]pyridazine is quite similar to 1,2,4,5-tetrazine and its derivatives even readily undergo inverse electron demand [4 + 2]-cycloadditions as bis-azadienes.[27,28]

Thus, coordination frameworks of bifunctional pyridazines could provide a unique opportunity for the evaluation of new types of supramolecular interactions, which arise from the electron deficient character of the heterocyclic frame. Particularly, the intriguing possibility for direct anion–π interaction was clearly recognized only recently,[29–31] it is relevant for negatively polarized atoms interacting with electron deficient aromatic systems (such as C_6F_6,[32,33] 1,3,5-triazine[34] and 1,2,4,5-tetrazine[35]) and it parallels the common and well known phenomenon of cation–π interactions and XH···π hydrogen bonding with electron rich aromatics.[36] Such interactions may be important for anion recognition and selective incorporation of certain anions from solution, while their potential for control over the structure of coordination frameworks themselves could be also significant,[37] as was proved by examination of 4,4′-bipyridazine and of pyridazino[4,5-*d*]pyridazine compounds.

Results and discussion

The compounds possess complex framework architectures based upon a combination of coordination preferences of the counterparts. The organic ligands generally adopt a tetradentate coordination mode, which is a readily-predictable feature of the system allowing rational design of the structures. In fact, the fused pyridazine ligand displays a pronounced affinity for silver(I) ions, as is reflected by the unusually high five- and six-fold AgN_5 and AgN_6 coordination.

Complexes with low nucleophilic anions

The framework structure of two isomorphous complexes $Ag_4(pp)_5(ClO_4)_4$ **1** and $Ag_4(pp)_5(SiF_6)(BF_4)_2{\cdot}4H_2O$ **2** is unique. In the chain-like array of the silver ions the adjacent centres are alternately doubly bridged (Ag–Ag 3.89 Å) by two and triply bridged (Ag–Ag 3.70 Å) by three pyridazine ligands completing unusual uniform five-fold coordination AgN_5 (Ag–N 2.36–2.56 Å) (Fig. 1, Table 1). This geometry is similar to the one found for the $AgPF_6$ complex with pyrazine (Ag–N 2.44 Å), the only precedent for pentacoordinate silver ions in complexes with non-chelating nitrogen donor ligands.[38] Each of the chains is linked to five close neighbours generating an unprecedented 3D architecture. The overall connectivity is an as yet unknown trinodal four- and five-connected framework, with the metal ions representing five- and the organic tetradentates as two kinds of four-connected nodes (total Schläfli symbol $\{4^2;6^4\}4\{4^2;6^2;8^2\}\{4^4;6^2;8^4\}4$). Simplification of the array in two dimensions, as interconnection of the chains with sets of the organic ligands led to a simple $3^2.4.3.4$ (snub square) tiling,[39] in which the triangles and squares (that appear in a 2 : 1 proportion) represent trigonal and tetragonal channels in real structures **1** and **2** (Fig. 2). Such a tiling pattern is usually related to the $CuAl_2$ structure.[40] However, any types of five-connected architectures are relatively rare,[38,41–45] and the tiling involving either five-connected nodes[45] or their duals, *i.e.* pentagonal motifs,[46] are very uncommon for metal–organic structures.

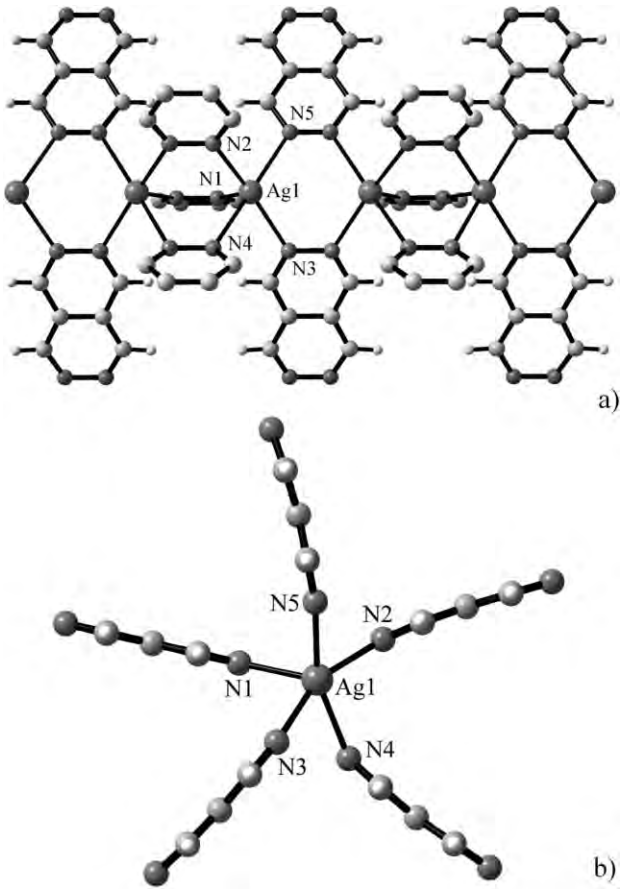

Fig. 1 Two views of the silver–pyridazine chain in **2**, which involves alternation of double and triple pyridazine bridges. AgN_5 coordination of the metal ions sustains five-fold interconnection of the chains.

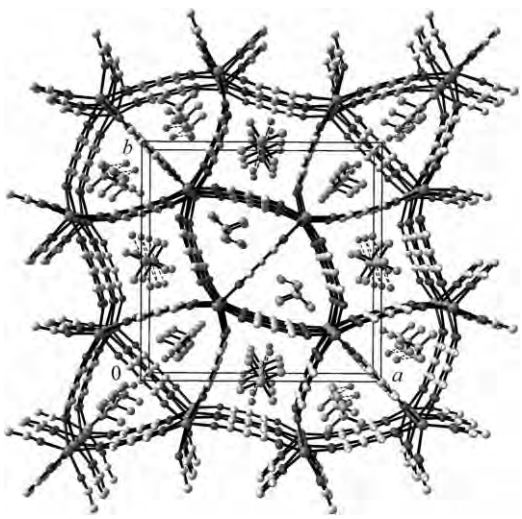

Fig. 2 Perspective view of five-connected framework **2**, showing two types of voids: tetragonal channels host SiF_6^{2-} anions, whereas trigonal channels are populated with BF_4^- anions.

Table 1 Selected bond lengths (Å) and angles (°) for **1–4**

$Ag_4(pp)_5(ClO_4)_4$ (**1**) (a: $1-y, 1-x, z$; b: $0.5-y, x-0.5, 0.5-z$)			
Ag(1)–N(1)	2.436(5)	N(1)–Ag(1)–N(2)	103.7(1)
Ag(1)–N(2)	2.472(4) × 2	N(2)–Ag(1)–N(2a)	84.8(2)
Ag(1)–N(3)	2.424(3) × 2	N(2)–Ag(1)–N(3b)	82.1(1)
N(1)–Ag(1)–N(3b)	94.3(1)		
$Ag_4(pp)_5(SiF_6)(BF_4)_2\cdot 4H_2O$ (**2**) (a: $x+0.5, 0.5-y, 0.5-z$; b: $1.5-x, y-0.5, 0.5-z$)			
Ag(1)–N(1)	2.447(4)	N(1)–Ag(1)–N(2)	109.0(2)
Ag(1)–N(2)	2.368(5)	N(1)–Ag(1)–N(3a)	89.0(2)
Ag(1)–N(3a)	2.358(5)	N(2)–Ag(1)–N(3a)	157.9(2)
Ag(1)–N(4)	2.561(6)	N(2)–Ag(1)–N(4)	85.0(2)
Ag(1)–N(5b)	2.449(5)	N(4)–Ag(1)–N(5b)	161.9(2)
$Ag_3(pp)_3(SO_3CF_3)_3\cdot H_2O$ (**3**) (a: $x+1/3, y+2/3, z-1/3$; b: $1-y, 1+x-y, z$; c: $2-x, 2+x-y, z$; d: $1.66-y, 1.33-x, z-1.66$)			
Ag(1)–N(1)	2.335(6) × 3	N(1)–Ag(1)–N(1b)	106.2(2)
Ag(1)–O(1)	2.39(2)	N(1)–Ag(1)–O(1)	112.6(2)
Ag(2)–N(2)	2.522(6) × 3	N(2)–Ag(2)–N(2b)	94.7(2)
Ag(2)–N(3)	2.531(6) × 3	N(2b)–Ag(2)–N(3d)	175.7(1)
Ag(3)–N(4)	2.320(6) × 3	N(4)–Ag(3)–N(4c)	105.9(2)
Ag(3)–O(1a)	2.58(2)	N(4)–Ag(3)–O(1a)	112.9(2)
$Ag_4(pp)_3(SiF_6)_2\cdot 10H_2O$ (**4**) (a: $1+x, y, z$; b: $x, y, z-1$)			
Ag(1)–N(1)	2.336(3)	N(1)–Ag(1)–N(3a)	125.1(1)
Ag(1)–N(3a)	2.270(3)	N(1)–Ag(1)–N(5)	92.6(1)
Ag(1)–N(5)	2.355(3)	N(5)–Ag(1)–N(3a)	134.0(1)
Ag(1)–O(1)	2.515(6)	N(1)–Ag(1)–O(1)	118.0(2)
Ag(2)–N(2)	2.299(3)	N(2)–Ag(2)–N(4a)	124.7(1)
Ag(2)–N(4a)	2.316(3)	N(2)–Ag(2)–N(6b)	113.2(1)
Ag(2)–N(6b)	2.354(3)	N(4a)–Ag(2)–N(6b)	106.3(1)
Ag(2)–O(2)	2.574(5)	N(2)–Ag(2)–O(2)	86.1(1)

Framework structure $Ag_3(pp)_3(SO_3CF_3)_3\cdot H_2O$ **3** reveals even higher metal–nitrogen coordination compared with **1** and **2**. It incorporates trinuclear units, in which two pairs of metal centers are triply bridged by three pyridazine ligands (Fig. 3), providing regular octahedral six-coordination for the central silver ion (Ag–N 2.52, 2.53 Å). Triple pyridazine bridges are characteristic for Cu(I) and Ag(I) compounds,[24–26] while spiro-annelation of such a motif is unprecedented. Each of the two outer silver ions coordinates also a water molecule, which is bridging between two trinuclear units. Thus the metal–organic portion of the structure

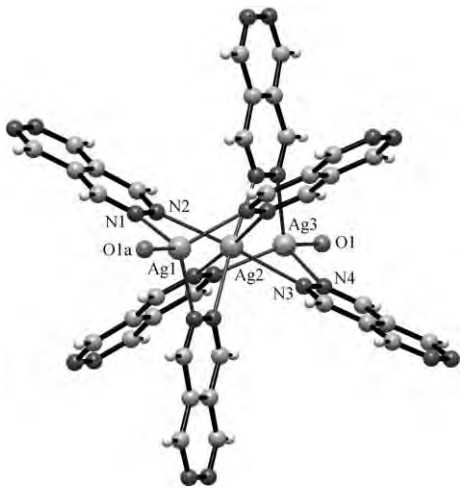

Fig. 3 Trinuclear silver–pyridazine cluster sustaining connectivity in complex **3**. Note unusual octahedral AgN_6 coordination of a central silver ion.

adopts a simple 3D octahedral motif (primitive cubic net "pcu")[47] (Fig. 4), and when the aqua bridges are also involved as the net links, the uninodal eight-connected topology "bcu" (body centered cubic net, which is usually related to CsCl or β-brass CuZn structure)[48] is found with the vertex symbol $\{4^{24};6^4\}$.

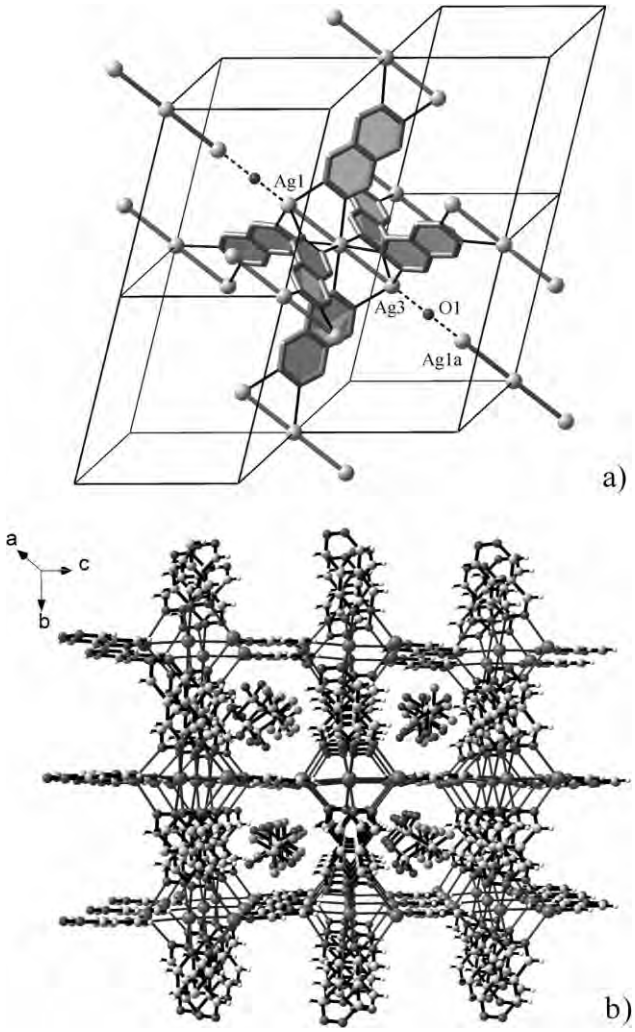

Fig. 4 Trinuclear silver–pyridazine clusters as the six-connected net points for primitive cubic motif in structure **3** and mode of an additional interconnection with bridging water molecules (a); perspective projection showing accommodation of triflate anions inside the channels (b).

The bipyridazine complex $Ag_3(bpdz)_3(SO_3CF_3)_3\cdot 2H_2O$ **9** has a very comparable framework architecture incorporating discrete trinuclear units (Fig. 5, Table 2). They are linked with a set of the organic ligands and bridging water molecules generating the same eight-connected "bcu" net, and the aqua bridges are actually collinear (Ag–O–Ag 166.4(1)°). An additional water molecule is involved in strong hydrogen bonding with counter anions and coordinated aqua ligands (O–O 2.68–2.78 Å). In the sense of the topology the trinuclear units in **3** and **9** are equal and they maintain the same overall connectivity, while the internal organization of the units is different owing to subtle features of the ligands. In the bipyridazine complex the central silver atom is tetracoordinated (two of the available nitrogen donors remain unused) and the present trimer may be regarded as a short fragment of the typical

Table 2 Selected bond lengths (Å) and angles (°) for **7–9**

$Ag_4(bpdz)_3(BF_4)_4\cdot H_2O$ (**7**) (a: $x-0.5, 0.5-y, z-0.5$; b: $1-x, 1-y, -z$; c: $1.5-x, y+0.5, 0.5-z$)			
Ag(1)–N(1)	2.299(3)	N(1)–Ag(1)–N(3a)	87.8(1)
Ag(1)–N(3a)	2.395(3)	N(1)–Ag(1)–N(6b)	144.2(1)
Ag(1)–N(6b)	2.225(3)	N(3a)–Ag(1)–N(6b)	122.3(1)
Ag(2)–N(2)	2.298(3)	N(2)–Ag(2)–N(5)	116.8(1)
Ag(2)–N(4c)	2.252(3)	N(2)–Ag(2)–N(4c)	118.7(1)
Ag(2)–N(5)	2.317(3)	N(5)–Ag(2)–N(4c)	124.2(1)
Ag(2)–F(1)	2.550(4)	N(2)–Ag(2)–F(1)	87.0(1)
$Ag_4(bpdz)_3(SiF_6)_2\cdot 3H_2O$ (**8**) (a: $-0.25+x, -0.25+y, 2-z$; b: $0.5-x, 0.5-y, 2-z$; c: $1.5-x, 0.5-y, 2-z$)			
Ag(1)–N(1)	2.269(4)	N(1)–Ag(1)–N(6c)	121.0(1)
Ag(1)–N(4a)	2.336(4)	N(1)–Ag(1)–N(4a)	123.4(1)
Ag(1)–N(6c)	2.295(4)	N(1)–Ag(1)–O(1b)	112.3(2)
Ag(1)–O(1b)	2.531(4)	N(3a)–Ag(2)–N(5)	137.8(1)
Ag(2)–N(2)	2.361(4)	N(3a)–Ag(2)–N(2)	122.3(1)
Ag(2)–N(3a)	2.210(4)	N(5)–Ag(2)–N(2)	96.3(1)
Ag(2)–N(5)	2.263(4)	N(3a)–Ag(2)–O(1)	107.1(2)
Ag(2)–O(1)	2.534(5)	N(2)–Ag(2)–O(1)	90.5(1)
$Ag_3(bpdz)_3(SO_3CF_3)_3\cdot 2H_2O$ (**9**) (a: $1-x, 0.5+y, 1-z$; b: $1+x, y, z$; c: $-x, 0.5+y, 2-z$; d: $x, y, z-1$)			
Ag(1)–N(1)	2.240(2)	N(1)–Ag(1)–N(3a)	149.7(1)
Ag(1)–N(3a)	2.242(2)	N(1)–Ag(1)–N(5)	112.07(8)
Ag(1)–N(5)	2.400(3)	N(3a)–Ag(1)–N(5)	95.56(9)
Ag(1)–O(1d)	2.747(2)	N(3a)–Ag(1)–O(1d)	101.42(8)
Ag(2)–N(2)	2.288(2)	N(2)–Ag(2)–N(9)	133.15(9)
Ag(2)–N(6)	2.358(2)	N(2)–Ag(2)–N(6)	111.53(9)
Ag(2)–N(7b)	2.373(2)	N(2)–Ag(2)–N(7b)	96.53(9)
Ag(2)–N(9)	2.288(3)	N(6)–Ag(2)–N(7b)	100.3(1)
Ag(3)–N(8b)	2.373(3)	N(10)–Ag(3)–N(11c)	141.7(1)
Ag(3)–N(10)	2.259(2)	N(10)–Ag(3)–N(8)	115.40(9)
Ag(3)–N(11c)	2.273(2)	N(11c)–Ag(3)–N(8)	96.82(9)
Ag(3)–O(1)	2.622(2)	N(8b)–Ag(3)–O(1)	110.14(8)

1 : 2 silver pyridazine helix found in $[Ag(pdz)_2](BF_4)$.[19] Six-fold coordination in the related complex **3** clearly suggests the higher donor ability of the electron deficient fused pyridazine towards silver ions, as may be compared with bipyridazine, the simple bifunctional analogue of the parent heterocycle. One example of AgN_6 coordination was found also for low-basic pyrazine.[38]

The ligands with double pyridazine sites offer even wider potential as a link between discrete polynuclear clusters, which themselves are very characteristic and predictable for pyridazine bridged silver(I) and copper(I) systems.[23,26] Thus a paradigmatic 4 : 6 silver/pyridazine aggregate affords a *para*-cyclophane like molecular frame involving a parallel stack of two silver–pyridazine dimers bridged by a pair of additional pyridazines (Scheme 2). This ensemble provides clearly distinguishable directions for propagation of the inherent molecular symmetry and therefore it

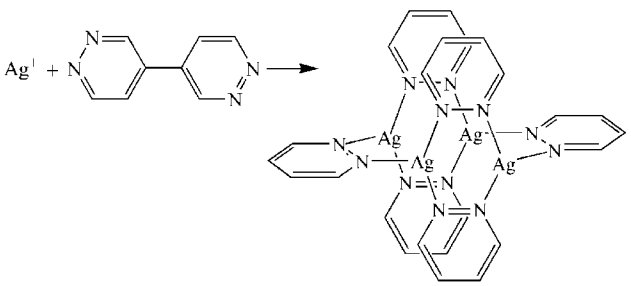

Scheme 2 Assembly of *para*-cyclophane like tetranuclear clusters sustaining structures **4**, **7** and **8**.

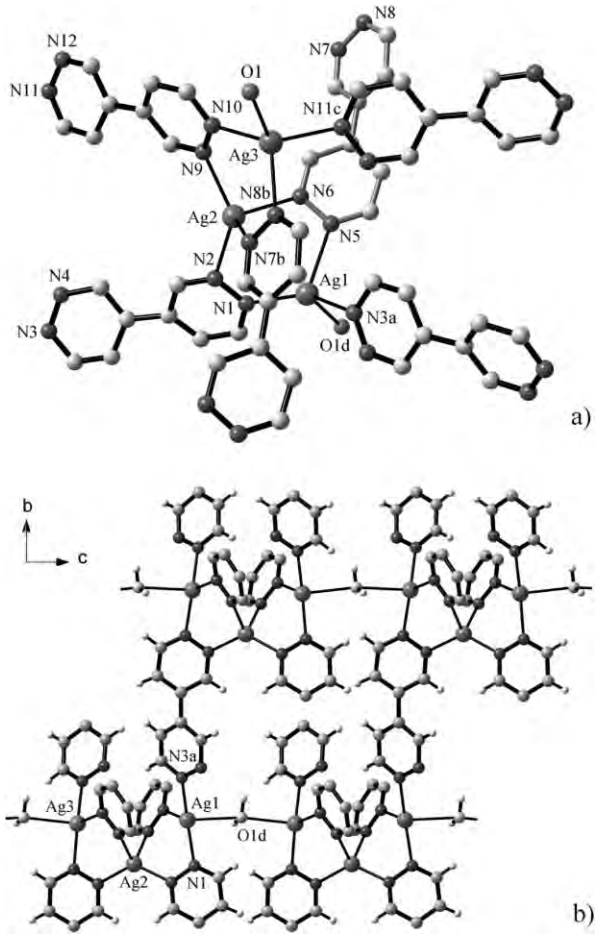

Fig. 5 Trinuclear silver–pyridazine clusters in structure **9** (a); fragment of the structure, which shows linear aqua bridges and tridentate bipyridazine molecules (b).

is perfectly suited as a "supramolecular synthon" for generation of framework solids. In fact, the structure of the tetranuclear synthon is greatly favorable since Ag···Ag contacts in the resulting Ag_4 square (3.28–3.51 Å) are consistent and complementary with typical parameters for slipped π/π stacking[49] and this facilitates the close and nearly parallel situation of two pairs of pyridazine rings (Table 2). Closely related compounds $Ag_4(pp)_3(SiF_6)_2\cdot 10H_2O$ **4**, $Ag_4(bpdz)_3(BF_4)_4\cdot H_2O$ **7** and $Ag_4(bpdz)_3(SiF_6)_2\cdot 3H_2O$ **8** uncover the potential of this approach (Table 3).

Table 3 Geometry of π···π contacts for cyclophane-like silver–pyridazine clusters in **4**, **7** and **8**[a]

Complex	*ccd*/Å	*ipd*/Å	*sc*/Å	*ipa*/°	*sa*/°
4	3.747(4)	3.418(3)	3.327(4)	3.30(4)	24.2(1)
7	3.915(3)	3.808(2)	3.340(3)	21.2(1)	13.4(1)
8	3.889(4)	3.756(3)	3.527(5)	13.9(1)	15.0(1)

[a] *ccd* is center-to-center distance (distance between ring centroids); *ipd* is interplanar distance (distance from one plane to the neighboring centroid); *sc* is a shortest contact to a neighboring plane; *ipa* is an interplanar angle and *sa* is a slippage angle (angle subtended by the intercentroid vector to the plane normal).

Despite the uniform silver–pyridazine linkage, the compounds demonstrate three distinct topologies related to the connector structure. Thus when two pyridazine functions are assembled by a symmetric *d*-edge annelation, as is present in planar pyridazino[4,5-*d*]pyridazine molecule, the framework structure **4** clearly follows the symmetry of the tetranuclear synthon. It exists as an evident planar (4,4)-net, in which one half of the links are represented by double bridges (Fig. 6). The coordination environment of two independent silver ions (AgN_3O and AgN_3O_2) was completed with distal water molecules (Ag–O 2.51–2.72 Å), while the SiF_6^{2-} counter anions are situated in the voids of the framework.

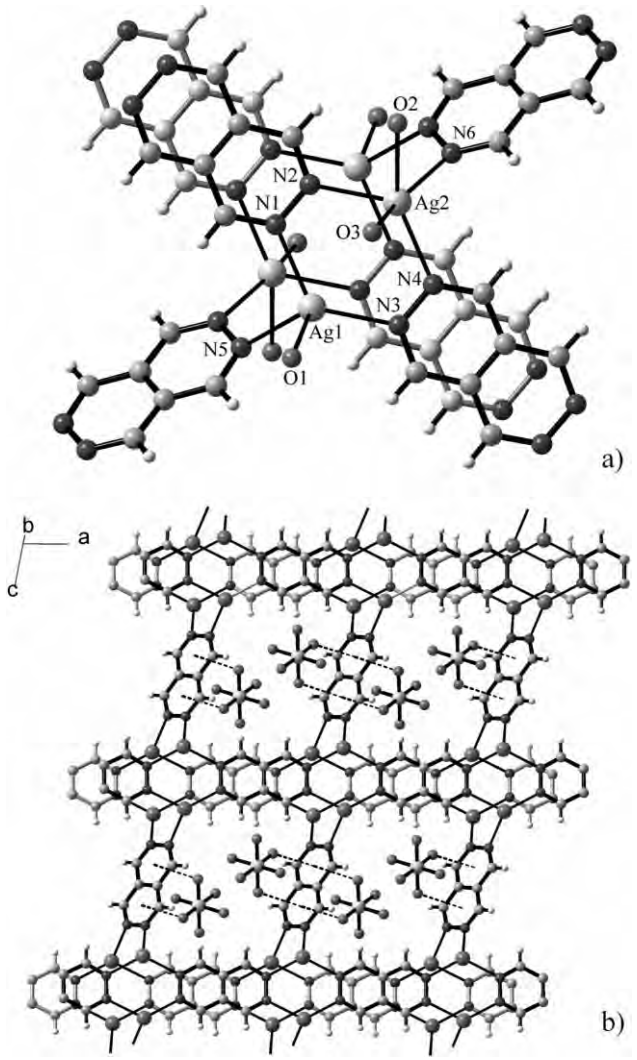

Fig. 6 Tetranuclear units in structure **4** (a) and the resulting 2D motif in the form of (4,4)-net composed with single and double organic bridges (b). An appreciable distortion of the tetramer structure is effected by high slippage angle in a π/π-stack of fused pyridazine molecules.

The same combination of single and double bridges supports interconnection of the silver tetramers in $Ag_4(bpdz)_3(SiF_6)_2\cdot 3H_2O$ **8** (Fig. 7). However, the entire framework is dominated by flexibility of the organic connector, and it adopts very rare 3D four-connected topology "lvt" (Schläfli symbol $\{4^2;8^4\}$).[50–52] Thus the 4,4′-bipyridazine tecton displays features of angular or conformational flexible connectors, similar to 4,4′-bipyrazoles,[8,52,53] 4,4′-bitriazole[54] and 4,4′-dipyridyldisulfide.[55] Pairs of bridging water molecules provide two further links between the tetramers and generation of an unprecedented uninodal six-connected topology with Schläfli symbol $\{4^{10};5^2;6^3\}$ (predicted by O'Keeffe and assigned the name "snk").[47]

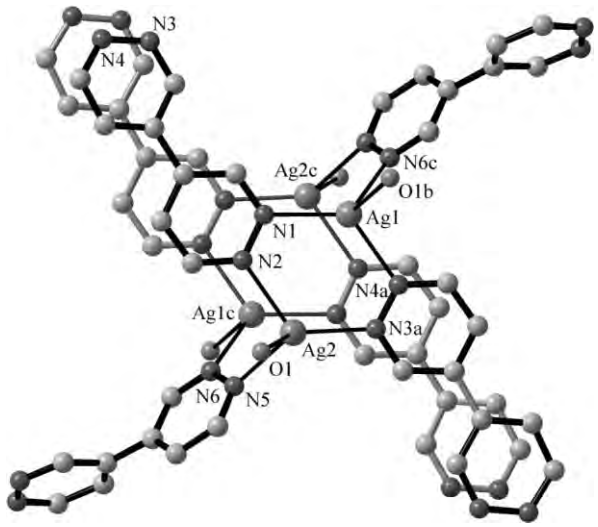

Fig. 7 Tetranuclear unit in structure **8**; it provides the same set of single and double bridging sites for four-connected net as in **4**, while the twisted conformation of the ligand predetermines mutual rotation of the adjacent tetramers and formation of a 3D framework.

Unlike these cases, the framework structure $Ag_4(bpdz)_3(BF_4)_4\cdot H_2O$ **7** was constituted with single organic bridges only, and thus each of six pyridazine sites at the tetranuclear synthon supports connectivity to a neighboring net vertex (Fig. 8). The resulting structure is two-dimensional and exists as a (3,6)-net. This is a first example of a planar six-connected net constructed with uniform ligand coordination and (3,6)-topology itself has a very scarce number of precedents.[54,56,57] The distorted tetrahedral environment of the silver ions is completed with distal fluorine atoms (Ag–F 2.55, 2.70 Å).

Carboxylate complexes

Complexes with fluorinated carboxylate anions R_F-COO^- reveal further design possibilities. Unlike BF_4^-, $SO_3CF_3^-$ and SiF_6^{2-} anions, the carboxylates are coordinated to the metal centers *via* both available oxygen atoms. Such bidentate acido groups are perfectly suited for sustaining bridging of two closely situated silver ions[58,59] and in this respect their coordination preferences are comparable with the pyridazine connectors, while the inductive effect of the R_F groups is essential for higher polarization of the Ag–O bonds and effective σ-donor Ag–N coordination (unlike essentially covalent copper(I) carboxylate dimers[60]). The tetradentate coordination of the bifuctional pyridazines allows efficient interconnection of the readily predictable 1D silver–carboxylate motifs with increase in the array dimensionality. Combination of these design prerequisites allows the rational construction of framework polymers, in which structure the pyridazine and carboxylate bridges efficiently cooperate as complementary components.

In the structure of $Ag_2(bpdz)(CF_3COO)_2\cdot 2/7CHCl_3$ **10** the bridging trifuoroacetate anions support a 1D silver–carboxylate

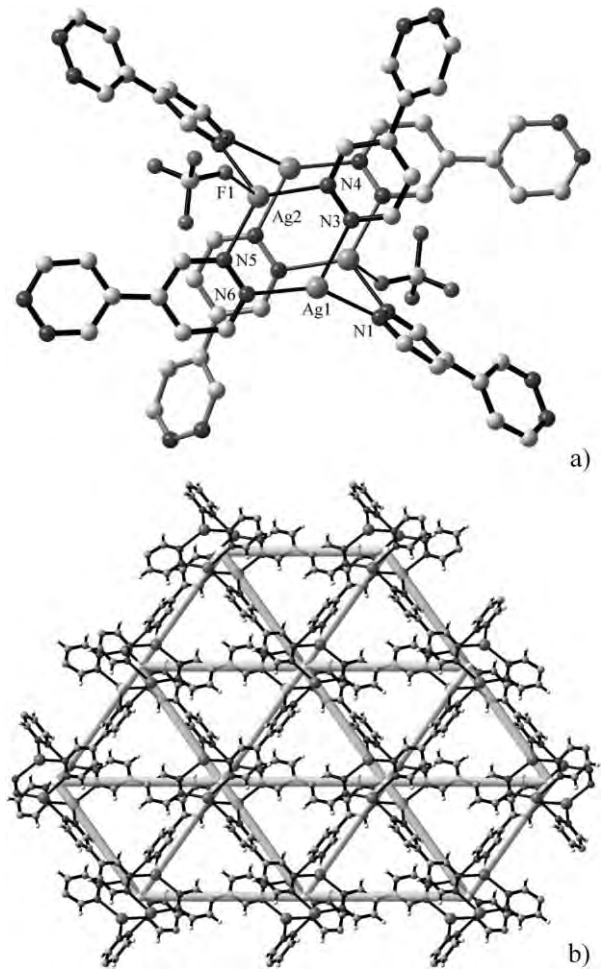

Fig. 8 Tetranuclear silver–pyridazine unit in **7** (a) as a six-connected vertex for a 2D framework of regular (3,6)-net topology (b).

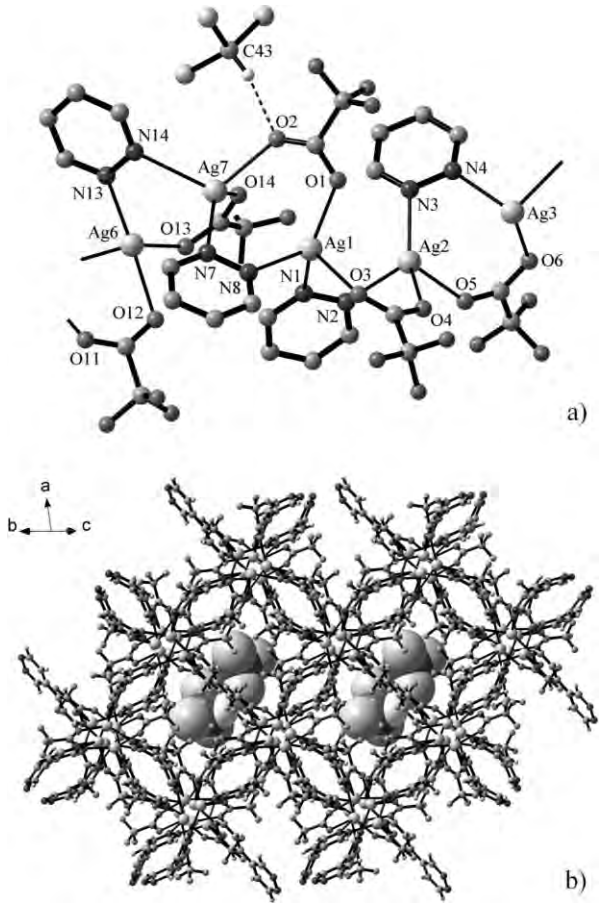

Fig. 9 Complementary bridging functions of pyridazine and carboxylate ligands for sustaining hybrid interconnection of the silver ions in structure **10** (a); resulting 3D framework with guest chloroform molecules located inside small cages (b).

linkage, which in the idealized form is a four-fold helix (Fig. 9, Table 4). The adjacent metal ions along the helix are interconnected with pyridazine bridges completing a distorted tetrahedral AgN_2O_2 coordination environment and thus the tetradentate bipyridazine ligands link a set of silver–trifluoroacetate helices into a 3D framework (helices of opposite chirality are present in equal proportions). However, a certain flexibility of the organic modules allows significant distortion of the framework (from the evident tetragonal symmetry) in order to minimize the volume of the crystal cages. The resulting structure thus possesses seven independent silver ions and provides only two little voids per unit cell with accessible space 2 × 127 Å^3 (or 8.0% of the crystal volume).[61] Each of the voids accommodates a guest molecule of chloroform, which has a comparable volume (*ca.* 130 Å^3) and forms CH···O hydrogen bonds to carboxyl oxygen atoms (H–O 2.16 Å; CHO 168°).

Fine-tuning of the shape and symmetry of 1D Ag/carboxylate/pyridazine substructure was possible even without alteration in connectivity of the metal ions and by simply varying the steric volume of the carboxyl substitutents. In complexes with higher fluorinated carboxylates $Ag_2(bpdz)(C_2F_5COO)_2$ **11** and $Ag_2(bpdz)(C_3F_7COO)_2$ **12** the silver/carboxylate portion adopts a geometry supporting the more distal mutual situation of perfluroalkyl groups and it exists as a three-fold helix. Further interconnection with bipyridazine linkers generates an evident trigonal motif, with uniform distorted tetrahedral AgN_2O_2 coordination (Fig. 10). C_2F_5 and C_3F_7 groups are directed towards the centre of the resulting hexagonal channels and completely fill any available space (free volume of the frameworks does not exceed 3.0%).[61] The frameworks possess a certain flexibility (the distance between axes of the neighboring helices is 9.05 and 10.16 Å for **11** and **12** respectively) and increase in the channel size allows situation of the larger C_3F_7 groups without any short contacts between the atoms.

Only structure $Ag(pp)(CF_3COO)$ **5** does not follow the proposed binding scheme, while at best it is suggestive of an intrinsic importance of the weak anion–π interactions discussed below. In this case the metal–pyridazine connectivity adopts 3D topology "lvt" (Schläfli symbol $\{4^2;8^4\}$),[50–52] with the metal ions and the organic tetradentates equally representing the planar four-connected nodes and the distorted octahedral coordination of the silver ions completed by terminal O,O-chelating carboxylate anions (Fig. 11). Any modification of the anion (for example, for pentafluoropropionate) is critical for the structure since this could prevent such special geometry favourable organization with the little rectangular channels of the framework filled with small CF_3 groups from the carboxylate ligands. In the structure of $Ag_2(pp)(C_2F_5COO)_2$ **6** the bridging carboxylate anions support a 1D silver–carboxylate linkage with additional interconnection

Table 4 Selected bond lengths (Å) and angles (°) for **5**, **6** and **10–12**

Ag(*pp*)(CF_3COO) (**5**) (a: x, 0.5 − y, z; b: 0.5 − x, 1 − y, z − 0.5; c: 0.5 − x, y − 0.5, z − 0.5)			
Ag(1)–N(1)	2.531(2) × 2	N(1)–Ag(1)–N(1a)	77.5(1)
Ag(1)–N(2)	2.448(2) × 2	N(1)–Ag(1)–N(2b)	86.47(8)
Ag(1)–O(1)	2.646(5) × 2	N(1)–Ag(1)–N(2c)	141.59(9)
N(1)–Ag(1)–O(1)	83.1(1)		
N(2c)–Ag(1)–O(1)	135.3(1)		
Ag_2(*pp*)($C_2F_5COO)_2$ (**6**) (a: 1.33 − y, 1.66 + x − y, z − 0.33; b: x − y + 2/3, x + 1/3, −z − 2/3)			
Ag(1)–N(1)	2.469(2)	N(1)–Ag(1)–N(2b)	107.81(7)
Ag(1)–N(2b)	2.259(2)	O(1)–Ag(1)–N(1)	104.74(7)
Ag(1)–O(1)	2.389(2)	N(1)–Ag(1)–O(2a)	88.17(7)
Ag(1)–O(2a)	2.255(2)	O(1)–Ag(1)–O(2a)	102.38(7)
O(1)–Ag(1)–N(2b)	99.02(7)		
Ag_2(*bpdz*)($CF_3COO)_2$·2/7$CHCl_3$ (**10**)			
Ag–N	2.251(3)–2.460(3)	O(4)–Ag(2)–N(2)	100.2(1)
Ag–O	2.227(3)–2.430(3)	N(3)–Ag(2)–N(2)	106.8(1)
N(5)–Ag(3)–N(4)	112.1(1)		
O(1)–Ag(1)–O(3)	96.0(1)	O(6)–Ag(3)–N(4)	98.2(1)
N(1)–Ag(1)–O(3)	104.5(1)	O(8)–Ag(4)–N(6)	116.4(1)
N(9)–Ag(4)–N(6)	100.3(1)		
Ag_2(*bpdz*)($C_2F_5COO)_2$ (**11**) (a: 1/3 − y, x − y + 2/3, z − 1/3)			
Ag(1)–N(1)	2.273(3)	N(1)–Ag(1)–O(1)	100.0(1)
Ag(1)–O(1)	2.382(3)	N(1)–Ag(1)–O(2a)	147.8(1)
Ag(1)–N(2a)	2.372(3)	N(1)–Ag(1)–N(2a)	108.3(1)
Ag(1)–O(2a)	2.291(3)	O(1)–Ag(1)–N(2a)	94.2(1)
O(1)–Ag(1)–O(2a)	102.7(1)		
Ag_2(*bpdz*)($C_3F_7COO)_2$ (**12**) (a: 1/3 − y, x − y − 1/3, z − 1/3; b: 2/3 − x + y, 1/3 − x, z + 1/3)			
Ag(1)–N(1)	2.362(3)	N(1)–Ag(1)–O(1)	97.8(1)
Ag(1)–N(2a)	2.266(3)	N(1)–Ag(1)–O(2b)	87.6(2)
Ag(1)–O(1)	2.405(4)	O(1)–Ag(1)–O(2b)	91.9(2)
Ag(1)–O(2b)	2.325(4)	N(1)–Ag(1)–N(2a)	118.0(1)
		O(1)–Ag(1)–N(2a)	101.6(1)

through pyridazine bridges and a uniform, distorted tetrahedral AgN_2O_2 coordination environment of the metal ions (Fig. 12). 1D coordination motifs exist in the form of three-fold helices, which are the same as observed for bipyridazine compounds **11** and **12**, and the resulting framework architecture is actually the same for all three compounds. Along the metal–organic helices, the compounds maintain short Ag–Ag contacts (3.05 Å for **11** and **12** and 3.18 Å for **6**) and thus the combination of anionic and pyridazine bridges forces the silver cations to approach each other. Comparable argentophilic interactions (2.97 Å) are known for the silver nitrate complex with 4,4′-bipyridine.[62,63]

Anion-π binding properties of the frameworks

Interaction of the non-coordinated anions (such as $SO_3CF_3^-$, SiF_6^{2-}) with the surface of the framework may occur by means of weak CH···X hydrogen bonding,[36] since the ligand frames provide multiple binding sites for such interactions. Thus, in Ag_3(*bpdz*)$_3(SO_3CF_3)_3$·$2H_2O$ **9** six types of weak hydrogen bonds CH···O were essential for crystal packing (C–O 3.21–3.31 Å, ∠CHO 150–173°), while the hydrogen bonding between the triflate anion and pyridazino[4,5-*d*]pyridazine in **3** was even stronger (C–O 3.06 Å; ∠CHO 157°).

However, the examined frameworks display much more peculiar and salient features of anion binding that is generally sustained rather by close direct interaction between the oxygen (fluorine)

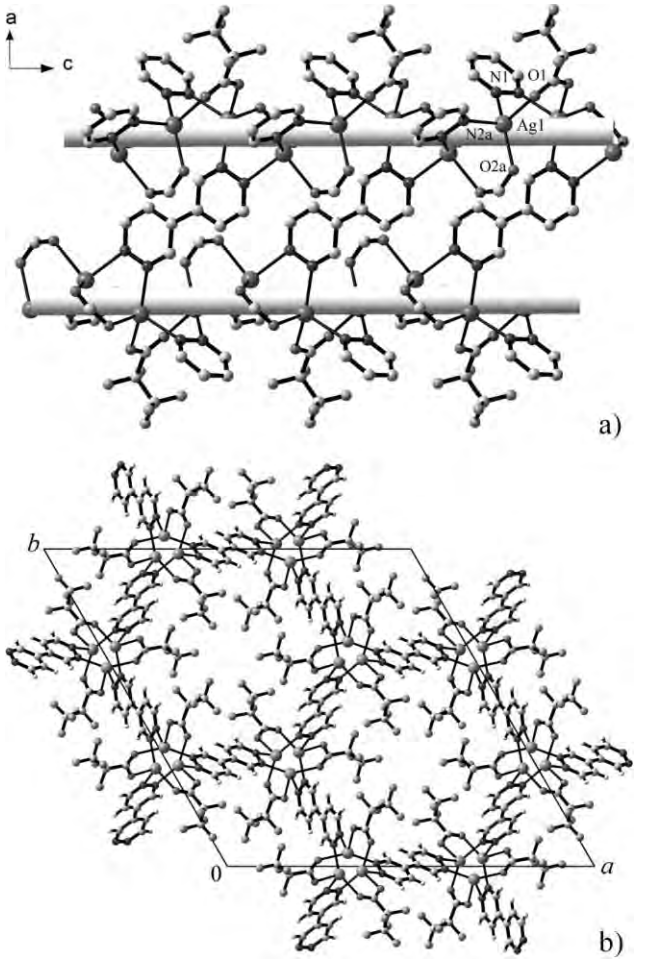

Fig. 10 Three-fold silver/carboxylate/pyridazine helices in structure **11** and their interconnection with tetradentate bipyridazine (a); projection of the resulting 3D framework down the *c* axis (direction of the helices) showing accommodation of the bulky C_2F_5 groups inside the hexagonal channels of the structure (b).

atoms and the aromatic π-cloud. The efficient anion–π interactions were especially common for the frameworks formed by fused bicyclic pyridazine, which reveals several unique features. Unlike any of hitherto reported examples, the fused pyridazine provides two closely situated and equally efficient sites for sustaining interactions with anions and this was reflected by unprecedented multiple anion–π,π binding.[64] The hexafluorosilicate complexes **2**, **4** and **8** are of special interest in this context: the geometry of octahedral SiF_6^{2-} anions (F–F *ca.* 2.40 Å) is perfectly complementary with the dimensions of fused bicyclic pyridazine (distance between the ring centroids is 2.43 Å) and this facilitates double F···π interactions between the components.

The structure of the mixed-anion complex **2** is highly illustrative since the available channels were filled in such a way that BF_4^- and SiF_6^{2-} anions (hydrogen bonded with water molecules) were accommodated within the trigonal and tetragonal channels respectively (Fig. 2). This appreciable discrimination of the channel population by shape and symmetry was predetermined by a set of very extensive interactions that occur between the anions and the aromatic "walls". Double SiF_6^{2-}–π,π interactions result in the formation of a π···A···π "anion–aromatic sandwich" (Fig. 13).

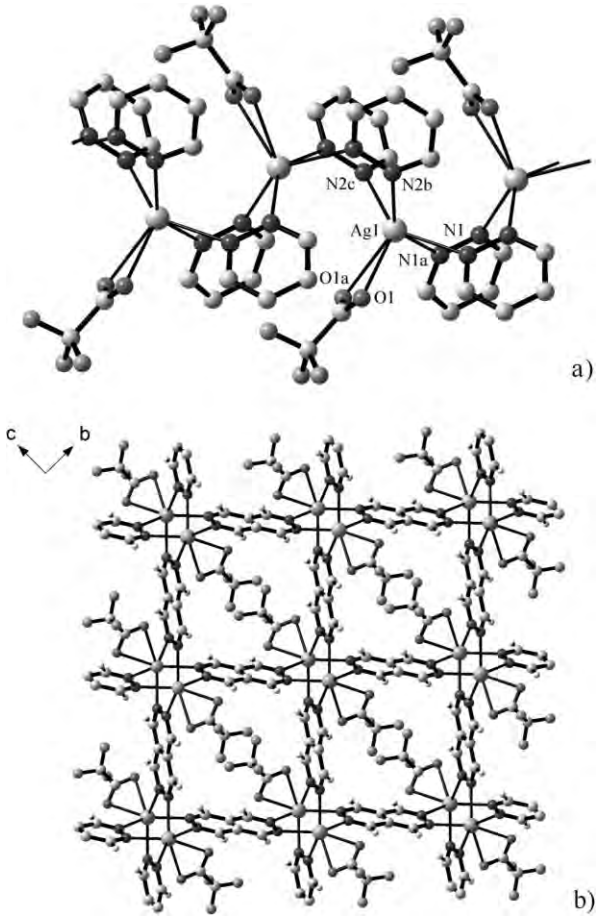

Fig. 11 Pyridazine bridged chain of silver atoms in structure **5** (a); projection of the structure down the *a* axis showing accommodation of the carboxylate groups inside tetragonal channels (b).

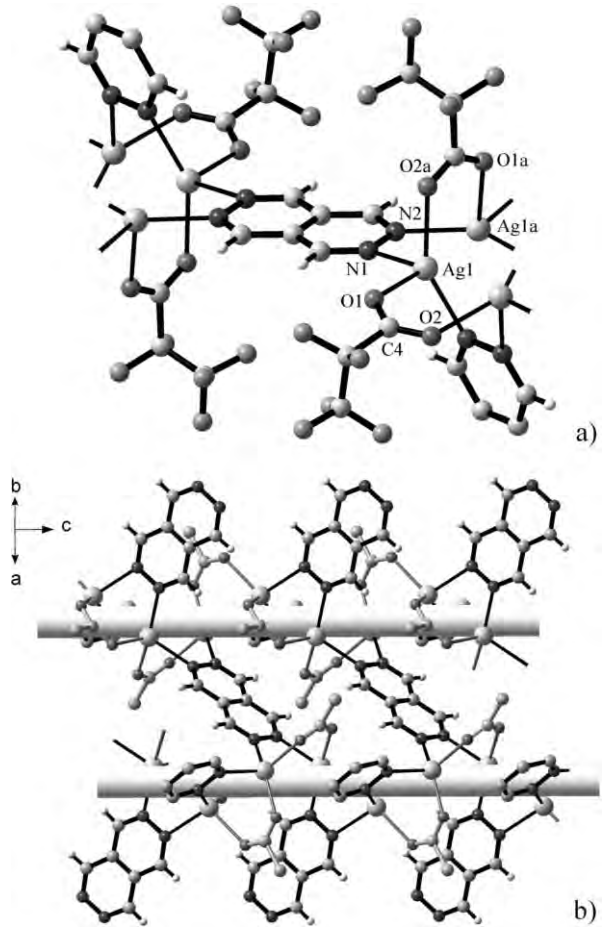

Fig. 12 Tetradentate function of the fused pyridazine ligand and coordination environment of the silver atoms in structure **6** (a); coordination motif in the form of three-fold helices (b) supports the same framework structure as in bipyridazine complexes **11**, **12**.

The fluorine atoms are situated at the short distances of 2.82 and 2.99 Å almost exactly above the ring centroids (angle of the F–π axis to the plane of the aromatic cycle 86.0 and 88.5°; Table 5). Such close anion–π interaction has very little literature precedents for derivatives of 1,2,4,5-tetrazine, the most electron deficient anion receptor.[37,65] That the fused pyridazine frame can support double interactions with the anions at both axial sides, allows postulation of even more complicated supramolecular architectures, such as the triple decker stack in the form of a

Table 5 Geometry of anion–π interactions with pyridazino[4,5-*d*]pyridazine[a]

				Distances/Å		
	Anion involved	Site	X–C(N) range/Å	X–π	X–plane	φ^b/°
1	ClO_4^{-c}	O(5)	2.99–3.31	2.838	2.810	81.9
		O(6)	3.16–4.11	3.410	3.105	65.6
2	BF_4^-	F(2)	3.33–3.49	3.053	3.052	88.5
		F(3)	3.23–4.04	3.399	3.156	68.2
	SiF_6^{2-}	F(5)	3.24–3.32	2.986	2.985	88.5
		F(6)	3.08–3.21	2.820	2.813	86.0
3	$SO_3CF_3^-$	O(3)	3.16–3.50	3.032	2.999	81.5
4	SiF_6^{2-}	F(1)	3.23–3.67	3.162	3.111	79.7
		F(2)	2.90–3.73	3.054	2.875	70.3
		F(4)	3.23–3.73	3.193	3.124	78.1
		F(5)	3.16–3.62	3.128	3.073	79.2
5	CF_3COO^-	F(1)	3.32–3.68	3.235	3.198	81.3
		F(2)	3.70–3.92	3.551	3.536	84.7

[a] For details see Fig. 13–15. [b] Angle of the X···centroid axis to the plane of aromatic cycle. [c] Mode of the interaction is similar to the one for BF_4^- anions in structure **2**.

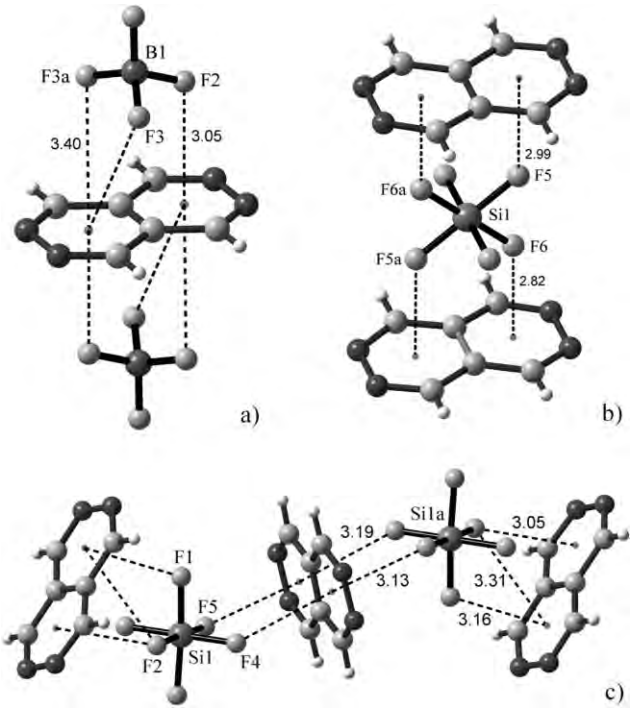

Fig. 13 Multiple anion–π interactions with a π-bifunctional fused pyridazine receptor: two types of anion–aromatic sandwiches in structure **2** (a, b) and triple-decker anion–aromatic club sandwiches in **4** (c).

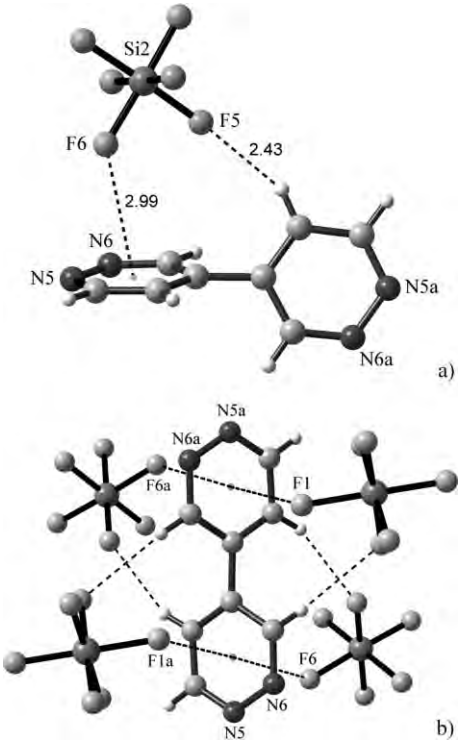

Fig. 14 Hydrogen bond (CH · · · F) assisted anion–π interaction in **8** (a); cooperative effect of four sets of such interactions maximizes the twist angle of bipyridazine molecule (b) and thus possibly influences a topology of the resulting coordination architecture.

π · · · A · · · π · · · A · · · π "club sandwich" generated in structure **4** (Fig. 13).

The dimensions of the BF_4^- anion (F–F *ca.* 2.12 Å) slightly mismatch the size of the receptor, and the closest interaction in **2** occurs in a different fashion, by stacking of the aromatic planes and triangular faces of the BF_4 tetrahedron leading to A · · · π · · · A "anion–aromatic sandwiches". The same type of interactions, with perchlorate anions, is present in structure **1**. However, the anions populating the tetragonal channels of the structure are disordered.

Despite of the very low nucleophility of the triflate anions, the characteristic anion–π interactions are important also for structure **3**, with remarkably close O · · · π contacts at 3.00 Å, while for the silver triflate complex with 4,4′-bipyridazine **9** the shortest separations of this type were appreciably longer (3.35 Å). This is consistent with the much higher LUMO energy of the pyridazine cycle *versus* the fused pyridazino[4,5-*d*]pyridazine,[27,28] and therefore with its weaker π-acidic properties. A similar conclusion was reached by Dunbar *et al.*[37] from comparison of bis-(2-pyridyl) substituted pyridazine and 1,2,4,5-tetrazine.

Nevertheless, it seems likely that the anion–π interactions with pyridazine may be also very efficient and could possess a sound structural significance. Thus, the structure of $Ag_4(bpdz)_3(SiF_6)_2 \cdot 3H_2O$ **8** demonstrates a quite unusual mode of anion–π binding that occurs with the assistance of weak hydrogen bonding. Each of four SiF_6^{2-} anions surrounding the bipyridazine molecule forms a close F · · · π contact at 2.988 Å (*i.e.* the pyridazine cycle unprecedentedly manifests π-acidity at either side of the ring, Fig. 14), while accepting a weak hydrogen bond from the adjacent heterocycle (F–C 3.30 and 3.51 Å; ∠CHF 155 and 170°). In this respect the functionalities and shapes of 4,4′-bipyridazine and the SiF_6^{2-} anions are complementary; cooperative effects of four pairs of such interactions force an unusually high twist angle between the two rings (63.0(1)° *vs.* 0–40° for any other *bpdz* structures). Such a twisted conformation of bipyridazine is most favorable for effective interaction with a set of four anions, while it dictates a specific orientation of the binding directions for the generation of the coordination framework and it is responsible for the unusual overall topology of **8**.

For negatively polarized fluorine atoms of CF_3 such interactions are much weaker. However, they were important for organizing the framework structure Ag(*pp*)(CF_3COO) **5**: each trifluoromethyl group is entrapped inside the "pocket" formed by pairs of fused pyridazines and the fluorine atoms maintain equally effective interactions to both aromatic sites (Fig. 15). The shortest F–π separations (3.24 Å) exceed the values for strong anion–π binding with the fused pyridazine (Table 4), and may be compared, for instance, with the O–π distance (3.20 Å) between 1,3,5-triazine and the nitrate anion.[34] Such illustrative intermolecular interactions that occur between the coordinated pyridazine and carboxylate ligands clearly contribute to the mutual orientation of the components and the entire supramolecular motif, while any lone pair · · · π binding itself has very little literature precedent, in particular it was involved as a stabilizing factor for sugar/nucleobase intramolecular interactions.[66,67]

Experimental

All chemicals were of analytical grade and used as received without further purification. Synthesis of pyridazino[4,5-*d*]pyridazine (by a laborious multi-step procedure) was first reported by Adembri,

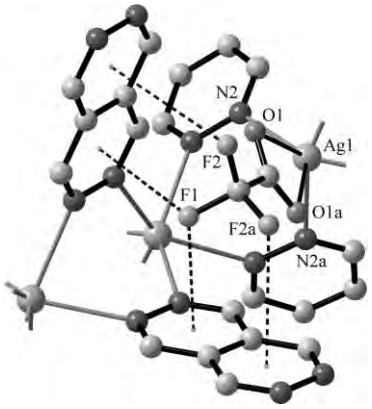

Fig. 15 Close interaction of the shape-complementary pyridazine and trifluoroacetate groups in structure **5**.

et al.[68] This method was poorly reproducible in our laboratory and therefore we have developed a novel one-pot synthesis following the methodology of "inverse electron demand Diels–Alder cycloadditon" of 1,2,4,5-tetrazine and acetylenedialdehyde tetraethylacetal, which possibly represents a general approach to a pyridazino[4,5-*d*]pyridazine frame[64] (Scheme 3). 4,4′-Bipyridazine was prepared in a similar fashion[69] using readily available (in a kilogram scale) *cis–trans*-1,4-bis-(dimethylamino)butadiene[70] as an extreme reactive "double dienophile". A very simple and efficient method for the preparation of unsubstituted 1,2,4,5-tetrazine was essentially a rational combination of two literature procedures.[71,72] Elemental analyses (C, H and N) were performed with a Perkin-Elmer 2400 analyzer. IR spectra were recorded with a UR-10 spectrometer (4000–400 cm^{-1}).

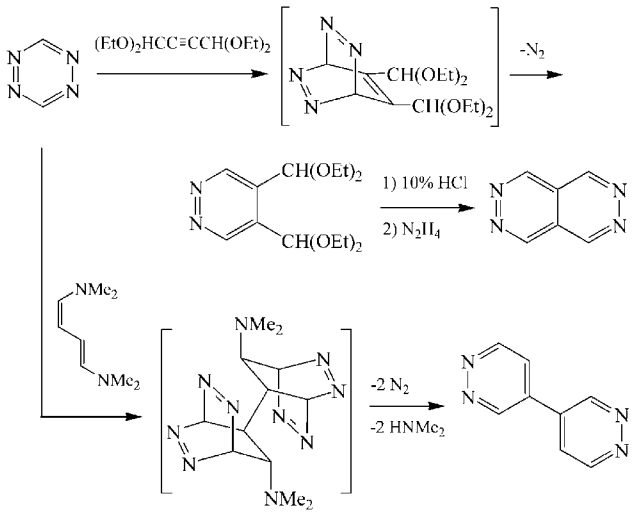

Scheme 3 Synthesis of bifunctional pyridazine ligands exploiting azadiene reactivity of 1,2,4,5-tetrazine.

Coordination compounds were synthesized by reacting the components in aqueous solution or by utilizing the layering technique in methanol–chloroform solution. Interaction of $AgBF_4$ and *pp* in usual glassware led to crystallization of a mixed-anion BF_4^-/SiF_6^{2-} complex (in a low yield of 20%) due to a partial hydrolysis of tetrafluoroborate and interaction of liberated HF with glass. The synthesis was reproduced also with a mixture of $AgBF_4$ and Ag_2SiF_6.

Preparation of $Ag_4(pp)_5(ClO_4)_4$ (1)

The ligand (0.020 g, 0.15 mmol) was added to a solution of 0.034 g (0.15 mmol) of $AgClO_4 \cdot H_2O$ in 3 mL of water and dissolved at 40–50 °C. The solution was filtered and slowly evaporated at r.t. for 5–6 d, after which the complex crystallized as yellow blocks (0.033 g, 75%). Anal. calcd for $C_{30}H_{20}Ag_4Cl_4N_{20}O_{16}$: C, 24.18; H, 1.35; N, 18.81. Found: C, 24.06; H, 1.44; N, 18.60%. Main IR absorption bands for **1** (cm^{-1}): 1310(w), 1290(w), 1255(m), 1145(s), 1120(s), 1090(s), 960(w), 895(w), 630(m), 480(m).

Complexes $Ag_3(pp)_3(SO_3CF_3)_3 \cdot H_2O$ (**3**, yellow prisms, 80%), $Ag_4(bpdz)_3(BF_4)_4 \cdot H_2O$ (**7**, faintly yellow prisms, 60%) and $Ag_3(bpdz)_3(SO_3CF_3)_3 \cdot 2H_2O$ (**9**) (colorless prisms, 60–70%) were prepared in the same fashion starting with silver triflate and tetrafluoroborate. Anal. calcd for $C_{21}H_{14}Ag_3F_9N_{12}O_{10}S_3$ (**3**): C, 21.28; H, 1.19; N, 14.18. Found: C, 21.41; H, 1.28; N, 14.37%. Main IR absorption bands for **3** (cm^{-1}): 1285(s), 1230(m), 1160(s), 1045(m), 955(w), 900(w), 645(s), 480(m). Anal. calcd for $C_{24}H_{20}Ag_4B_4F_{16}N_{12}O$ (**7**): C, 22.67; H, 1.59; N, 13.22. Found: C, 22.80; H, 1.52; N, 13.38%. Anal. calcd for $C_{27}H_{22}Ag_3F_9N_{12}O_{11}S_3$ (**9**): C, 25.31; H, 1.73; N, 13.12. Found: C, 25.44; H, 1.69; N, 13.40%. Main IR absorption bands for **9** (cm^{-1}): 1595(w), 1345(m), 1285(s), 1270(s), 1180(m), 1055(s), 865(m), 650(m), 530(w).

Preparation of $Ag_4(pp)_3(SiF_6)_2 \cdot 10H_2O$ (4)

A hot solution of $Ag_2SiF_6 \cdot 4H_2O$ (0.086 g, 0.2 mmol) in 2 mL of water was added to a hot solution of the ligand (0.040 g, 0.3 mmol) in 3 mL of water. An additional 4 mL of water were added and the mixture was heated at 95 °C for dissolution of the initially formed yellow precipitate. After slow cooling to room temperature yellow crystals were formed. They were separated by filtration, washed with methanol, diethyl ether and dried. The yield was 45%. Anal. calcd for $C_{18}H_{32}Ag_4F_{12}N_{12}O_{10}Si_2$: C, 16.73; H, 2.50; N, 13.01. Found: C, 16.92; H, 2.34; N, 13.08%. Main IR absorption bands for **4** (cm^{-1}): 1310(m), 1290(m), 1255(s), 1175(w), 960(w), 900(w), 765(s), 485(s).

Under the same conditions 4,4′-bipyridazine produces light-yellow $Ag_4(bpdz)_3(SiF_6)_2 \cdot 3H_2O$ (**8**) (50%), while yellow prisms of $Ag_4(pp)_5(SiF_6)(BF_4)_2 \cdot 4H_2O$ (**2**) were obtained in a 70% yield reacting the ligand and a 1 : 1 mixture of silver tetrafluoroborate and hexafluorosilicate. Anal. calcd for $C_{30}H_{28}Ag_4B_2F_{14}N_{20}O_4Si$ (**2**): C, 24.35; H, 1.91; N, 18.93. Found: C, 24.48; H, 1.78; N, 19.07%. Anal. calcd for $C_{24}H_{24}Ag_4F_{12}N_{12}O_3Si_2$ (**8**): C, 23.17; H, 1.94; N, 13.51. Found: C, 23.34; H, 1.81; N, 13.64%. Main IR absorption bands for **8** (cm^{-1}): 3470(m), 1585(w), 1340(m), 975(m), 870(m), 760(s), 700(w), 490(s).

Preparation of $Ag_{14}(bpdz)_7(CF_3COO)_{14} \cdot 2CHCl_3$ (10)

Crystals of the compound were obtained using a layering technique. In a typical synthesis, a solution of 0.044 g (0.2 mmol) $AgCF_3COO$ in 4 mL MeOH was layered over a solution of 0.019 g (0.12 mmol) of 4,4′-bipyridazine in 2 mL MeOH and 3 mL $CHCl_3$. Slow interdiffusion of the layers, in a 10–15 d period, led to crystallization of the complex (0.025 g, 40% yield) as large light yellow prisms. Anal. calcd for $C_{86}H_{44}Ag_{14}Cl_6F_{42}N_{28}O_{28}$: C, 23.27;

H, 1.00; N, 8.84. Found: C, 23.45; H, 1.14; N, 9.01%. Main IR absorption bands for **10** (cm^{-1}): 1705(s), 1445(w), 1330(w), 1220(s), 1135(s), 975(w), 850(m), 815(m), 735(m).

Compounds Ag(*pp*)(CF_3COO) (**5**), Ag_2(*pp*)($C_2F_5COO)_2$ (**6**), Ag_2(*bpdz*)($C_2F_5COO)_2$ (**11**) and Ag_2(*bpdz*)($C_3F_7COO)_2$ (**12**) were synthesized in a similar way (50–70% yields), starting with the corresponding silver salts. Anal. calcd for $C_8H_4AgF_3N_4O_2$ (**5**): C, 27.22; H, 1.14; N, 15.87. Found: C, 27.53; H, 1.17; N, 15.98%. Main IR absorption bands for **5** (cm^{-1}): 1685(s), 1435(m), 1310(w), 1295(w), 1250(m), 1215(s), 1140(s), 960(w), 895(w), 845(m), 810(w), 485(m). Anal. calcd for $C_{12}H_4Ag_2F_{10}N_4O_4$ (**6**): C, 21.38; H, 0.60; N, 8.32. Found: C, 21.29; H, 0.77; N, 8.67%. Main IR absorption bands for **6** (cm^{-1}): 1680(s), 1410(w), 1335(m), 1250(m), 1215(m), 1165(s), 1030(m), 820(w), 480(w). Anal. calcd for $C_{14}H_6Ag_2F_{10}N_4O_4$ (**11**): C, 24.02; H, 0.86; N, 8.01. Found: C, 23.95; H, 1.01; N, 8.28%. Main IR absorption bands for **11** (cm^{-1}): 1685(s), 1420(w), 1340(s), 1255(s), 1215(s), 1175(s), 1035(m), 825(w), 740(m). Anal. calcd for $C_{16}H_6Ag_2F_{14}N_4O_4$ (**12**): C, 24.02; H, 0.76; N, 7.01. Found: C, 23.86; H, 0.89; N, 7.18%. Main IR absorption bands for **12** (cm^{-1}): 1700(s), 1415(w), 1345(m), 1230(s), 1125(m), 1100(w), 975(m), 875(w), 825(w), 750(w).

Crystallography

Crystal data and refinement details are given in Tables 6 and 7. Crystallographic measurements for **1–3** and **7** were made at 213 K using a Stoe Imaging Plate diffraction system and for the other compounds with a Siemens SMART CCD area-detector diffractometer (empirical absorption corrections using SADABS).[73] The structures were solved by direct methods and refined in the anisotropic approximation using SHELXS-97 and SHELXL-97.[74,75] The hydrogen atoms were included at idealized positions (CH 0.96 Å) and then refined as riding, with $U_{iso}(H) = 1.2U_{eq}(C)$. For **2–4** and **7** the hydrogen atoms of the water molecules were not included, while for **8** and **9** they were located and then treated as riding with $U_{iso}(H) = 1.5U_{eq}(O)$.

Complexes **1** and **2** were actually isostructural. However, refinement of **2** in the tetragonal space group $P4_2/mnm$ was not successful and led to poor convergence with a total disorder in the region of the anions, while systematically $F_o^2 > F_c^2$ values were highly suggestive of twinning. A satisfactory model of pseudo-merohedral twinning, with equal contributions of the components, was found for orthorhombic space group *Pnnm* and this afforded a suitably-refinable model. Structure **3** is actually centrosymmetric. However, refinement in space group $R\bar{3}c$ was not satisfactory and it led to a total disorder in the region of the $CF_3SO_3^-$ anions. A realistic ordered model was found for acentric space group *R*3*c* and the structure was refined as a racemic twin [Flack *x* parameter 0.42(6)].

In structure **12** the heptafluoropropyl group of the anion was disordered over two positions with partial occupancy factors 0.6 and 0.4, the disorder was resolved with restraints in geometry of the CF linkage and in *U* values for the C and F atoms of the disordered fragment. As well, a set of geometry restraints was applied to resolve disorder for one of two unique BF_4^- anions in structure **7** and a typical "rotational" disorder for two of seven unique trifluoroacetate groups in **10**. Possible disorder of the pentafluoroethyl group in **11** was reflected by high *U* values; however, it was not possible to resolve the disordering scheme,

Table 6 Crystal data and structure refinement for pyridazino[4,5-*d*]pyridazine complexes $Ag_4(pp)_5(ClO_4)_4$ (**1**), $Ag_4(pp)_5(SiF_6)(BF_4)_2\cdot 4H_2O$ (**2**), $Ag_3(pp)_3(SO_3CF_3)_3\cdot H_2O$ (**3**), $Ag_4(pp)_3(SiF_6)_2\cdot 10H_2O$ (**4**), Ag(*pp*)(CF_3COO) (**5**) and Ag_2(*pp*)($C_2F_5COO)_2$ (**6**)

	1	2	3	4	5	6
Formula	$C_{30}H_{20}Ag_4Cl_4N_{20}O_{16}$	$C_{30}H_{28}Ag_4B_2F_{14}N_{20}O_4Si$	$C_{21}H_{14}Ag_3F_9N_{12}O_{10}S_3$	$C_{18}H_{32}Ag_4F_{12}N_{12}O_{10}Si_2$	$C_8H_4AgF_3N_4O_2$	$C_{12}H_4Ag_2F_{10}N_4O_4$
M	1449.88	1479.91	1185.23	1292.22	353.02	673.93
T/K	213	213	213	273	293	213
Crystal system	Tetragonal	Orhtorhombic	Trigonal	Monoclinic	Orthorhombic	Trigonal
Space group	$P4_2/nmm$	*Pnnm*	*R*3*c*	$P2_1/c$	*Pnma*	$R\bar{3}$
Z	2	2	6	2	4	9
a/Å	17.008(1)	17.080(1)	15.6887(9)	8.8507(1)	7.3514(2)	25.281(1)
b/Å	17.008(1)	17.078(1)	15.6887(9)	17.2093(3)	12.5897(3)	25.281(1)
c/Å	7.8591(5)	7.5920(7)	24.4805(18)	12.0859(2)	11.3054(3)	7.4007(4)
β/°				100.785(1)		
V/Å^3	2273.3(2)	2214.6(3)	5218.2(6)	1808.34(5)	1046.34(5)	4096.3(3)
μ(Mo-Kα)/cm^{-1}	20.19	18.94	19.72	23.30	19.70	22.81
D_{calc}/g cm^{-3}	2.118	2.219	2.263	2.373	2.241	2.459
θ_{max}/°	26.01	26.72	27.87	30.51	30.50	28.28
Refl. collected	10426	5722	10789	14014	4178	9710
Indep. refl.	1238	2364	2695	5420	1535	2208
Indep. refl. > 2σ(*I*)	877	1870	1790	4543		
R_{int}	0.031	0.036	0.038	0.021	0.017	0.025
Parameters refined	115	184	176	263	88	145
*R*1, *wR*2 [*I* > 2σ(*I*)]	0.031, 0.088	0.042, 0.119	0.031, 0.077[a]	0.046, 0.114	0.029, 0.070	0.024, 0.062
*R*1, *wR*2 [all data]	0.044, 0.092	0.051, 0.123	0.050, 0.081	0.055, 0.118	0.035, 0.074	0.032, 0.064
Max, min peak/e Å^{-3}	1.36, −0.44	1.38, −0.74	1.23, −0.86	1.37, −1.14	0.85, −0.84	0.65, −0.53

[a] Flack parameter $x = 0.42(6)$.

Table 7 Crystal data and structure refinement for 4,4′-bipyridazine complexes $Ag_4(bpdz)_3(BF_4)_4{\cdot}H_2O$ (**7**), $Ag_4(bpdz)_3(SiF_6)_2{\cdot}3H_2O$ (**8**), $Ag_3(bpdz)_3(SO_3CF_3)_3{\cdot}2H_2O$ (**9**), $Ag_{14}(bpdz)_7(CF_3COO)_{14}{\cdot}2CHCl_3$ (**10**), $Ag_2(bpdz)(C_2F_5COO)_2$ (**11**) and $Ag_2(bpdz)(C_3F_7COO)_2$ (**12**)

	7	8	9	10	11	12
Formula	$C_{24}H_{20}Ag_4B_4F_{16}N_{12}O$	$C_{24}H_{24}Ag_4F_{12}N_{12}O_3Si_2$	$C_{27}H_{22}Ag_3F_9N_{12}O_{11}S_3$	$C_{86}H_{44}Ag_{14}Cl_6F_{42}N_{28}O_{28}$	$C_{14}H_6Ag_2F_{10}N_4O_4$	$C_{16}H_6Ag_2F_{14}N_4O_4$
M	1271.24	1244.21	1281.36	4438.37	699.97	799.99
T (K)	213	273	213	273	293	273
Crystal system	Monoclinic	Orthorhombic	Monoclinic	Triclinic	Trigonal	Trigonal
Space group	$P2_1/n$	$Fddd$	$P2_1$	$P\bar{1}$	$R\bar{3}$	$R\bar{3}$
Z	2	16	2	1	9	9
a/Å	10.6823(8)	7.7384(2)	8.7652(6)	13.9023(2)	26.9862(2)	28.4273(2)
b/Å	12.1323(7)	38.1690(8)	22.100(2)	14.4405(3)	26.9862(2)	28.4273(2)
c/Å	14.6844(9)	50.807(1)	10.4417(7)	18.2666(2)	7.6176(1)	7.5353(1)
α/°	90	90	90	107.079(1)	90	90
β/°	97.017(8)	90	91.874(1)	111.592(1)	90	90
γ/°	90	90	90	94.2320(1)	120	120
V/Å^3	1888.9(2)	15006.6(6)	2021.6(2)	3190.46(9)	4804.32(8)	5273.54(9)
μ(Mo-Kα)/cm^{-1}	21.65	22.29	17.07	23.62	19.50	18.15
D_{calc}/g cm^{-3}	2.235	2.203	2.105	2.310	2.177	2.267
θ_{max}/°	27.88	28.28	29.02	27.48	28.70	28.68
Refl. collected	17163	18785	17561	43985	22279	22669
Indep. refl.	4457	4586	8866	14474	2753	3002
Indep. refl. $> 2\sigma(I)$	3545	3893	8301			
R_{int}	0.035	0.028	0.016	0.026	0.027	0.025
Parameters refined	316	259	586	973	154	262
$R1$, $wR2$ [$I > 2\sigma(I)$]	0.034, 0.090	0.048, 0.132	0.021, 0.050[a]	0.033, 0.074	0.039, 0.112	0.046, 0.151
$R1$, $wR2$ [all data]	0.043, 0.092	0.056, 0.136	0.023, 0.050	0.047, 0.079	0.049, 0.119	0.053, 0.157
Max, min peak/e Å^{-3}	1.90, −1.03	2.50, −0.83	0.40, −0.57	1.93, −2.25	0.86, −1.01	0.89, −0.78

[a] Flack parameter $x = 0.02(1)$.

while for the sake of overall convergence the atoms were refined anisotropically with restraints in the geometry of the C_2F_5 group.

Graphical visualisation of the structures was made using the program DIAMOND[76] and the topological analysis was performed using program OLEX.[77]

Conclusions

Silver(I) coordination polymers are very illustrative of the general principles for crystal design, and they reveal a variety of framework architectures originated in the propagation of typical silver–pyridazine coordination motifs. We believe that the readily available and inexpensive bifunctional pyridazines could possess even higher significance for the supramolecular synthesis of framework solids, as may be compared with the prototypal 4,4′-bipyridines and pyridazines. The ligands unite the potential of the latter families and they may be best applicable for bridging of paramagnetic metal ions and generation of polynuclear magnetic materials, design of open metal–organic frameworks and ion-exchange materials. The unique combination of pronounced π-acidity and σ_N-donor ability, as was established for fused bicyclic pyridazino[4,5-*d*]pyridazine, suggests its wider potential for functionalization of hydrophobic crystal cavities and development of molecular and polymeric metal–organic species with special anion binding properties. The system manifests an unprecedented double anion–π,π binding and demonstrates a key structural prototype for anion selective interactions of electron deficient polycycles.

Acknowledgements

The work was in part supported by a grant from Deutsche Forschungsgemeinschaft UKR 17/1/06 (HK and KVD).

References

1 C. Janiak, *Dalton Trans.*, 2003, 2781.
2 C. J. Kepert, *Chem. Commun.*, 2006, 695.
3 S. Kitagawa, S. Noro and T. Nakamura, *Chem. Commun.*, 2006, 701.
4 B. Moulton and M. J. Zaworotko, *Chem. Rev.*, 2001, **101**, 1629.
5 M. Eddaoudi, D. B. Moler, H. Li, B. Chen, T. M. Reineke, M. O'Keeffe and O. M. Yaghi, *Acc. Chem. Res.*, 2001, **34**, 319.
6 A. Y. Robin and K. M. Fromm, *Coord. Chem. Rev.*, 2006, **250**, 2127.
7 S. Noro, S. Kitagawa, M. Kondo and K. Seki, *Angew. Chem., Int. Ed.*, 2000, **39**, 2082.
8 E. B. Rusanov, V. V. Ponomarova, V. V. Komarchuk, H. Stoeckli-Evans, E. Fernandez-Ibañez, F. Stoeckli, J. Sieler and K. V. Domasevitch, *Angew. Chem., Int. Ed.*, 2003, **42**, 2499.
9 P. J. Hagrman, D. Hagrman and J. Zubieta, *Angew. Chem., Int. Ed.*, 1999, **38**, 2638.
10 A. B. Descalzo, R. Martínez-Máñez, F. Sancenón, K. Hoffmann and K. Rurack, *Angew. Chem., Int. Ed.*, 2006, **45**, 5924.
11 X.-L. Wang, C. Qin, E.-B. Wang, Z.-M. Su, L. Xu and S. R. Batten, *Chem. Commun.*, 2005, 4789.
12 L. Pan, X. Liu, X. Lei, X. Huang, D. H. Olson, N. J. Turro and J. Li, *Angew. Chem., Int. Ed.*, 2003, **42**, 542.
13 H. Chun, D. Kim, D. N. Dybtsev and K. Kim, *Angew. Chem., Int. Ed.*, 2004, **43**, 971.
14 D. Li, T. Wu, X.-P. Zhou, R. Zhou and X.-C. Huang, *Angew. Chem., Int. Ed.*, 2005, **44**, 4175.
15 M. Munakata, L. P. Wu and T. Kuroda-Sowa, *Adv. Inorg. Chem.*, 1999, **46**, 173–303.
16 A. N. Khlobystov, A. J. Blake, N. R. Champness, D. A. Lemenovskii, A. G. Majouga, N. V. Zyk and M. Schröder, *Coord. Chem. Rev.*, 2001, **222**, 155.
17 S. M. Cortez and R. G. Raptis, *Coord. Chem. Rev.*, 1998, **169**, 363.

18 L. Plasseraud, H. Maid, F. Hampel and R. W. Saalfrank, *Chem.–Eur. J.*, 2001, **7**, 4007.
19 L. Carlucci, G. Ciani, D. M. Proserpio and A. Sironi, *Inorg. Chem.*, 1998, **37**, 5941.
20 P. V. Solntsev, J. Sieler, H. Krautscheid and K. V. Domasevitch, *Dalton Trans.*, 2004, 1153.
21 D. R. Whitcomb and R. D. Rogers, *Inorg. Chim. Acta*, 1997, **256**, 263.
22 D. R. Whitcomb and R. D. Rogers, *J. Chem. Crystallogr.*, 1995, **25**, 137.
23 H. V. Rasika Dias, H. V. K. Diyabalanage and C. S. Palehepitiya Gamage, *Chem. Commun.*, 2005, 1619.
24 A. S. Batsanov, M. J. Begley, M. W. George, P. Hubberstey, M. Munakata, C. E. Russel and P. H. Walton, *J. Chem. Soc., Dalton Trans.*, 1999, 4251.
25 M. J. Begley, P. Hubberstey, C. E. Russel and P. H. Walton, *J. Chem. Soc., Dalton Trans.*, 1994, 2483.
26 M. Maekawa, M. Munakata, T. Kuroda-Sowa and Y. Nozaka, *J. Chem. Soc., Dalton Trans.*, 1994, 603.
27 N. Haider, *Tetrahedron*, 1991, **47**, 3959.
28 N. Haider, *Acta Chim. Slov.*, 1994, **41**, 205.
29 Ya. S. Rosokha, S. V. Lindeman, S. V. Rosokha and J. K. Kochi, *Angew. Chem., Int. Ed.*, 2004, **43**, 4650.
30 S. Demeshko, S. Dechert and F. Meyer, *J. Am. Chem. Soc.*, 2004, **126**, 4508.
31 A. Frontera, F. Saczewski, M. Gdaniec, E. Dziemidowicz-Borys, A. Kurland, P. M. Deya, D. Quiñonero and C. Garau, *Chem.–Eur. J.*, 2005, **11**, 6560.
32 J. P. Gallivan and D. A. Dougherty, *Org. Lett.*, 1999, **1**, 103.
33 M. Raimondi, G. Calderoni, A. Famulari, L. Raimondi and F. Cozzi, *J. Phys. Chem. A*, 2003, **107**, 772.
34 P. U. Maheswari, B. Modec, A. Pevec, B. Kozlevčar, C. Massera, P. Gamez and J. Reedijk, *Inorg. Chem.*, 2006, **45**, 6637.
35 C. Garau, D. Quiñonero, A. Frontera, A. Costa, P. Ballester and P. M. Deyà, *Chem. Phys. Lett.*, 2003, **370**, 7.
36 G. R. Desiraju and T. Steiner, *The Weak Hydrogen Bond in Structural Chemistry and Biology*, Oxford University Press Inc., New York, 1999.
37 B. L. Schottel, H. T. Chifotides, M. Shatruk, A. Chouai, L. M. Perez, J. Bacsa and K. R. Dunbar, *J. Am. Chem. Soc.*, 2006, **128**, 5895.
38 L. Carlucci, G. Ciani, D. M. Proserpio and A. Sironi, *Angew. Chem., Int. Ed. Engl.*, 1995, **34**, 1895.
39 B. Grünbaum and G. C. Shephard, *Tilings and Patterns*, W. H. Freeman and Company, New York, 1987.
40 M. O'Keeffe and B. G. Hyde, *Crystal Structures I. Patterns and Symmetry*, Mineralogical Society of America, Washington, DC, 1996, p. 165.
41 S. R. Batten, B. F. Hoskins and R. Robson, *New J. Chem.*, 1998, **22**, 173.
42 L. Pan, B. S. Finkel, X. Y. Huang and J. Li, *Chem. Commun.*, 2001, 105.
43 D. L. Long, A. J. Blake, N. R. Champness, C. Wilson and M. Schröder, *J. Am. Chem. Soc.*, 2001, **123**, 3401.
44 V. V. Ponomarova, V. V. Komarchuk, I. Boldog, A. N. Chernega, J. Sieler and K. V. Domasevitch, *Chem. Commun.*, 2002, 436.
45 X.-H. Bu, W. Weng, J.-R. Li, W. Chen and R.-H. Zhang, *Inorg. Chem.*, 2002, **41**, 413.
46 B. Moulton, J. Lu and M. J. Zaworotko, *J. Am. Chem. Soc.*, 2001, **123**, 9224.
47 Reticular Chemistry Structure Resource, URL http://rcsr.anu.edu.au, website accessed May 9, 2007.
48 T.-T. Luo, H.-L. Tsai, S.-L. Yang, Y.-H. Liu, R. D. Yadav, C.-C. Su, C.-H. Ueng, L.-G. Lin and K.-L. Lu, *Angew. Chem.*, 2005, **117**, 6217.
49 C. Janiak, *J. Chem. Soc., Dalton Trans.*, 2000, 3885.
50 B. Rather, B. Moulton, R. D. B. Walsh and M. J. Zaworotko, *Chem. Commun.*, 2002, 694.
51 L. Carlucci, N. Cozzi, G. Ciani, M. Moret, D. M. Proserpio and S. Rizzato, *Chem. Commun.*, 2002, 1354.
52 I. Boldog, E. B. Rusanov, A. N. Chernega, J. Sieler and K. V. Domasevitch, *J. Chem. Soc., Dalton Trans.*, 2001, 893.
53 J. He, Y.-G. Yin, T. Wu, D. Li and X.-C. Huang, *Chem. Commun.*, 2006, 2845.
54 A. B. Lysenko, E. V. Govor, H. Krautscheid and K. V. Domasevitch, *Dalton Trans.*, 2006, 3772.
55 R. Horikoshi and T. Mochida, *Coord. Chem. Rev.*, 2006, **250**, 2595.
56 C.-Y. Su, Y.-P. Cai, C.-L. Chen and B.-S. Kang, *Inorg. Chem.*, 2001, **40**, 2210.
57 E. Y. Lee, S. Y. Jang and M. P. Suh, *J. Am. Chem. Soc.*, 2005, **127**, 6374.
58 X.-M. Chen and T. C. W. Mak, *J. Chem. Soc., Dalton Trans.*, 1991, 1219.
59 T. C. W. Mak, W.-H. Yip, C. H. L. Kennard, G. Smith and E. J. O'Reilly, *Aust. J. Chem.*, 1986, **39**, 541.
60 A. Toth, C. Floriani, A. Chiesti-Villa and C. Guastini, *Inorg. Chem.*, 1987, **26**, 236.
61 A. L. Spek, *J. Appl. Crystallogr.*, 2003, **36**, 7.
62 F. Robinson and M. J. Zaworotko, *J. Chem. Soc., Chem. Commun.*, 1995, 2413.
63 O. M. Yaghi and H. Li, *J. Am. Chem. Soc.*, 1996, **118**, 295.
64 I. A. Gural'skiy, P. V. Solntsev, H. Krautscheid and K. V. Domasevitch, *Chem. Commun.*, 2006, 4808.
65 B. L. Schottel, J. Basca and K. R. Dunbar, *Chem. Commun.*, 2005, 46.
66 S. Sarkhel, A. Rich and M. Egli, *J. Am. Chem. Soc.*, 2003, **125**, 8998.
67 I. Berger and M. Egli, *Chem.–Eur. J.*, 1997, **3**, 1400.
68 G. Adembri, F. De Sio, R. Nesi and M. Scotton, *Chem. Commun. (London)*, 1967, 1006.
69 K. V. Domasevitch, I. A. Gural'skiy, P. V. Solntsev, E. B. Rusanov, H. Krautscheid, J. A. K. Howard and A. N. Chernega, *Dalton Trans.*, 2007, 3140.
70 M. F. Fegley, N. M. Bortnick and C. H. McKeever, *J. Am. Chem. Soc.*, 1958, **79**, 4140.
71 A. T. M. Marcelis and H. C. Van Der Plas, *J. Heterocycl. Chem.*, 1987, **24**, 545.
72 J. Sauer, D. K. Heldmann, J. Hetzenegger, J. Krauthan, H. Sichert and J. Schuster, *Eur. J. Org. Chem.*, 1998, 2885.
73 G. M. Sheldrick, *SADABS Area-Detector Absorption Correction, 2.03*, University of Göttingen, Göttingen, Germany, 1999.
74 G. M. Sheldrick, *SHELX97, A system of computer programs for X-ray structure determination*, University of Göttingen, Göttingen, Germany, 1997.
75 G. M. Sheldrick, *Acta Crystallogr., Sect. A*, 1990, **46**, 467.
76 K. Brandenburg, *Diamond 2.1c*, Crystal Impact GbR, Bonn, 1999.
77 O. V. Dolomanov, A. J. Blake, N. R. Champness and M. Schröder, *J. Appl. Crystallogr.*, 2003, **36**, 1283.